JOURNAL OF CATALYSIS 74, 240–251 (1982)

Surface Characterization of the $Ru_3(CO)_{12}/Al_2O_3$ System

II. Structure and Reactivity of the Surface Carbonylic Complexes

E. GUGLIELMINOTTI AND A. ZECCHINA

Istituto di Chimica Fisica, Università di Torino, Corso M. d'Azeglio 48, 10125 Torino, Italy

AND

A. BOSSI AND M. CAMIA

Istituto "G. Donegani" S.p.A., Via G. Fauser 4, 28100 Novara, Italy

Received May 22, 1981; revised November 11, 1981

The structure of the anchored carbonylic complexes (Ru_A, Ru_B, and Ru_C) formed by interaction of $Ru_3(CO)_{12}$ with Al_2O_3 is further investigated by ^{13}CO–^{12}CO isotopic substitution. All complexes contain two coupled CO oscillators per ruthenium centre and the local structure is tetrahedral (Ru_A) or octahedral (Ru_B and Ru_C). The reactivity of these species towards simple molecules is also tested and the interconversion of the Ru_B and Ru_C species in reducing and oxidizing atmospheres is established. The oxidation states III, II, and 0 are proposed for Ru in the Ru_A, Ru_B, and Ru_C species, respectively.

INTRODUCTION

In Part I (*1*) we have shown that by interaction of $Ru_3(CO)_{12}$ with hydrated alumina, new well-defined carbonylic species are formed whose concentration depends upon the pretreatment conditions. These species (which cannot be extracted from the surface with solvents) can be considered as true anchored compounds where the ruthenium atoms are in a different oxidation state. Due to their potential interest as possible catalytic centres, it is important to define in as detailed a way as possible their structure and reactivity. In particular in this paper the following points are investigated: (i) the number of CO ligands per Ru centre; (ii) the reactivity towards simple molecules (H_2, O_2, NO, Py, NH_3, H_2O, CO); (iii) interconversion among the species.

EXPERIMENTAL

Sample preparation, sample designations, and spectroscopic measurements are the same as those described in Part I (*1*).

Temperature-programmed reduction (TPR) experiments have been carried out in a conventional apparatus similar to that described by Robertson *et al.* (*2*) equipped with a mass flow controller, Matheson model 8240. The reducing mixture was 5% H_2 and 95% Ar and the flow rate 40 cm^3/min.

RESULTS

^{13}CO–^{12}CO Exchange Experiments

Figure 1 illustrates the effect of isotopic ^{13}CO substitution on the ir spectrum of a Ru_A complex (bands at 2138 and 2175 cm^{-1}). The experiment has been carried out as follows. A 0.33% sample fully decarbonylated *in vacuo* at 623 K has been contacted with ^{12}CO (5.3 kPa) to form the characteristic A pair. Then ^{13}CO has been bled into the gas in order to produce a gradual change in the ^{13}CO–^{12}CO ratio in the gas phase in contact with the sample, the ir spectrum being taken at fixed intervals of time. It can be seen that an exchange slowly takes place. In fact the original

0021-9517/82/040240-12$02.00/0
Copyright © 1982 by Academic Press, Inc.
All rights of reproduction in any form reserved.

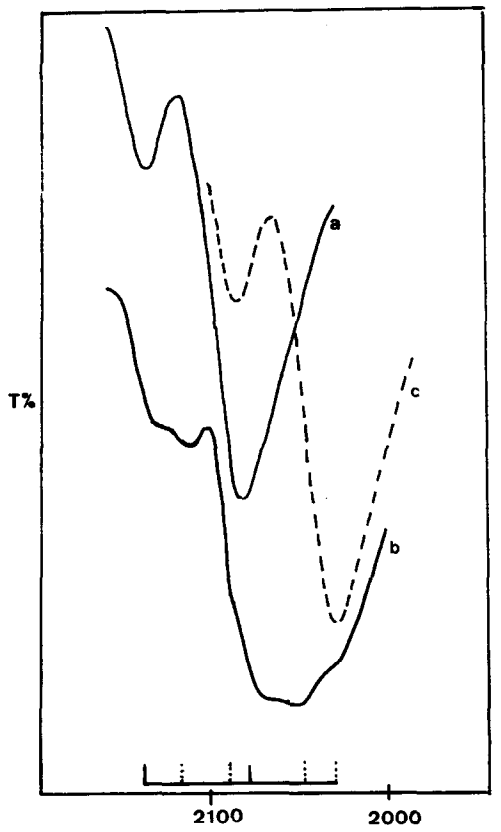

FIG. 1. Curve a: initial spectrum of ^{12}CO (5.3 kPa) adsorbed on a 0.33% sample decarbonylated *in vacuo;* spectrum b taken at intermediate $^{13}CO/^{12}CO$ exchange ratio; spectrum c corresponds to ^{13}CO (5.3 kPa). In the lower part of the figure the solid and dotted marks represent the experimental and calculated frequencies.

bands tend to decrease while others develop at lower frequencies. Although the exact $^{13}CO-^{12}CO$ ratio is not known, the observed trend is clear enough to be interpreted in terms of the superposition of bands due to partially or totally exchanged Ru_A complexes.

Figure 2 shows a similar experiment carried out on an R sample for the B pair, the only difference being represented by the exchange temperature, which is ~373 K in this case. The original bands again gradually decrease in intensity. At intermediate exchange ratios six bands are clearly visible, while after nearly complete exchange, only two absorptions at lower frequencies (2022 and 1960 cm^{-1}) are observed. A similar experiment has not been carried out on the C pair because it was not strictly necessary: in fact it will be shown below that the C pair belongs to a simple well-defined dicarbonylic complex on the basis of reduction experiments only.

The Reactivity of the Ru_A Complexes

As shown in Part I, the A pair is partially removed by outgassing at room temperature (RT) and is completely eliminated around 400 K, i.e., the CO ligands are weakly bonded and the complex is stable only in CO atmosphere. This fact represents a strong limitation for reactivity experiments, as the presence of gaseous CO complicates the situation. As a consequence a limited number of experiments

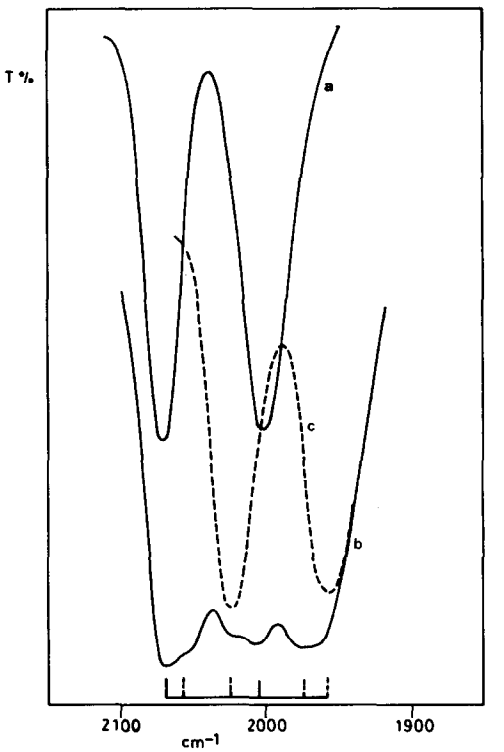

FIG. 2. Spectrum a: Ru_B (^{12}CO) species. Spectra b and c taken at intermediate and total exchange ratios, respectively. In the lower part of the figure the solid and dotted marks represent the experimental and calculated frequencies.

have been carried out and in this section we shall only illustrate the reactivity towards O_2, H_2O, and NO. In addition, in order to elucidate the problem of the oxidation state of ruthenium, the preferential formation of Ru_A complexes on oxidized samples will be illustrated.

At RT oxygen has no effect on the A pair in equilibrium with 13.3 Pa CO: by increasing the temperature to 423 K, the CO bands simultaneously disappear (experiment not shown for the sake of brevity), i.e., the complex can be oxidized.

The effect of water (and of other bases like NH_3, Py) is stronger: by exposure to the saturated vapour of H_2O, the A pair disappears already at RT. This effect is reversible: in fact if water is removed by prolonged outgassing at RT, the A pair can be partly reformed by exposure to 5.3 kPa CO (experiment not shown).

The effect of NO is illustrated in Fig. 3. The solid curve represents the spectrum of a 1.57% sample previously decarbonylated at 623 K, then contacted with CO. The two characteristic bands of the A pair represent the main feature of the spectrum. It is evident that the low-frequency component is strongly asymmetric on the low-frequency side, suggesting the presence of a broad component in the range 2050–1950 cm^{-1}. Exposure to NO (5.3 kPa) causes spectro-

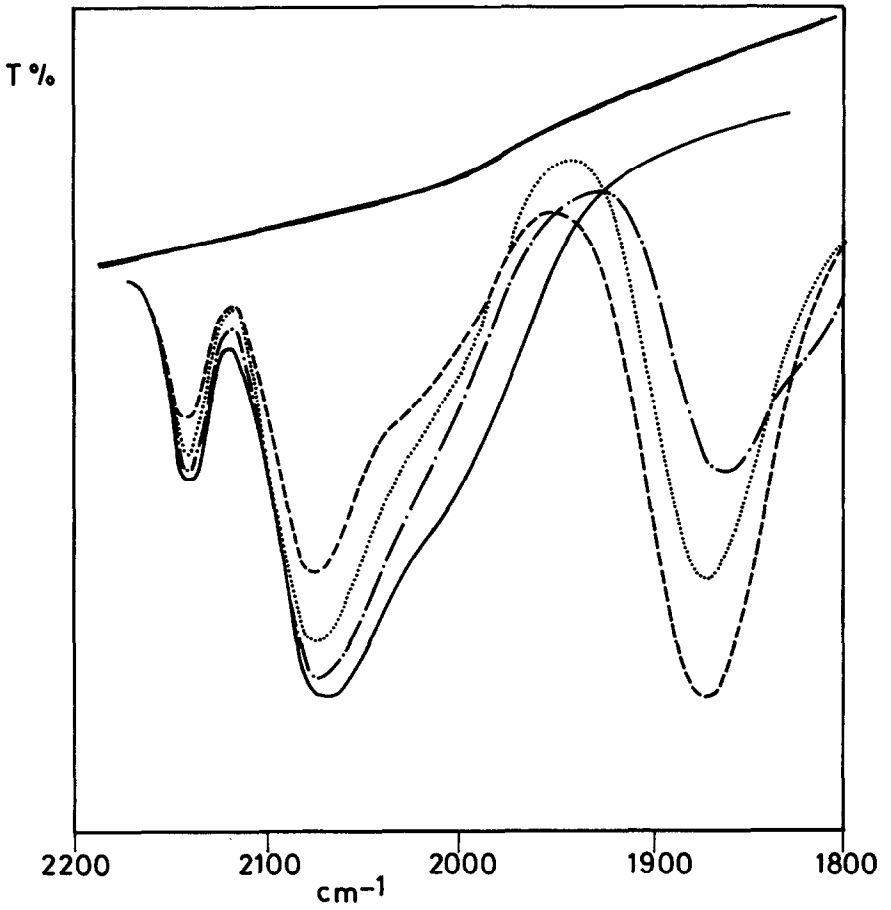

FIG. 3. Upper solid curve: background after decarbonylation at 623 K *in vacuo* of a 1.57% sample; solid curve: after CO adsorption; dot-dashed curve: after the first NO dose (133 Pa); dotted and dashed curves: spectra taken at successive stages of interaction.

scopic changes in the ranges 2150–1950 (carbonylic) and 1900–1800 cm^{-1} (nitrosylic). *Range 2150–1960 cm^{-1}*: (i) immediately after the NO contact a preferential erosion of the broad absorption in the range 2050–1950 cm^{-1} is observed; (ii) for increasing contact times and pressures the A pair progressively disappears; *range 1900–1800 cm^{-1}*: (i) immediately after the NO contact a band is observed at 1840 cm^{-1} together with a shoulder at 1810 cm^{-1}; (ii) for increasing contact times the shoulder at ~1810 cm^{-1} disappears while a band at 1873 cm^{-1} undergoes a progressive intensity enhancement which is proportional to the simultaneous decrement of the A pair bands.

This experiment can be partly reversed. If, after NO evacuation, the sample is contacted again with CO at 373 K, the 1873-cm^{-1} band decreases and the A pair is partly restored. The proportionality between the decrement of the A pair and the increment of the 1873-cm^{-1} band suggests a ligand displacement reaction where the NO ligands displace the CO ligands and form surface nitrosylic structures.

However, this is probably not the only process occurring on the surface: in the low-frequency range (1600–1100 cm^{-1}: not shown for the sake of brevity) new bands appear which monitor the formation of oxidation products of CO, caused by a parallel oxidative interaction of NO with adsorbed CO.

In Fig. 4 the contact of CO (5.3 kPa) with a 1.57% decarbonylated sample previously exposed to O_2 (5.3 kPa) at 423 K is illustrated. The A pair is immediately formed with high intensity (curve b) together with pronounced bands in the range 1700–1200 cm^{-1} (curve b'). All bands tend to increase with time (curves c, d, c', d'). It is noticeable that in the range 2150–1900 cm^{-1} not only is the A pair present but also a large and ill-defined absorption at lower frequencies ($2070 \geq \tilde{\nu} \geq 1900$) (curve b) is ob-

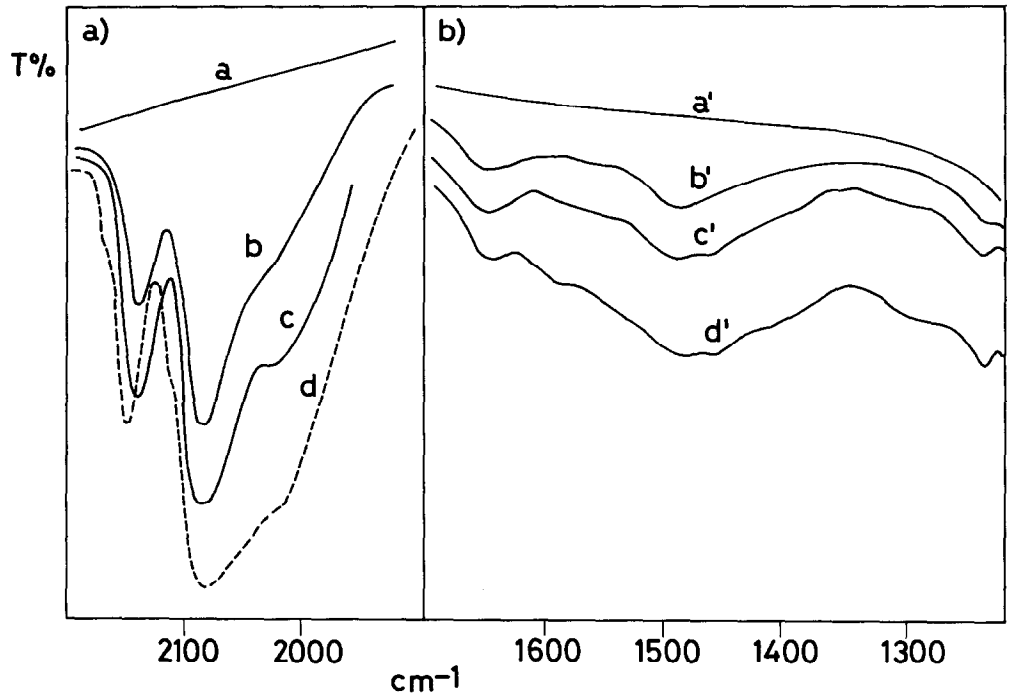

FIG. 4. a and a': background after oxidation at 423 K (1.57% sample); spectra b, b'; c, c'; and d, d' taken at increasing contact times of 5.3 kPa CO.

served. By increasing the temperature to 423 K, the situation becomes increasingly complex as the low-frequency absorption further develops, showing a well-defined shoulder at 2020 cm^{-1} which strongly resembles the spectrum of CO adsorbed on a 1.57% sample (decarbonylated *in vacuo*) (Fig. 7 of Part I). In the meantime the bands in the range 1650–1100 cm^{-1} become even stronger, while those of the A pair have reached their maximum intensity. A moderate temperature increase up to 473 K (not reported in the figure) causes a decrease of the A pair and a further increment of the absorption in the range 2070–1950 cm^{-1}.

The oxidation state of the ruthenium after oxygen adsorption at 423 K is easily revealed by a TPR experiment carried out on a sample treated in the same way (Fig. 5a). It can be seen that a narrow peak occurs at 433 K, nearly coincident with that observed for pure RuO_2 (Fig. 5b), and the peak area corresponds to the reduction of Ru^{IV} to Ru^0. These facts clearly show that after oxidation at 423 K the ruthenium is in a RuO_2-like form. All the ir manifestations

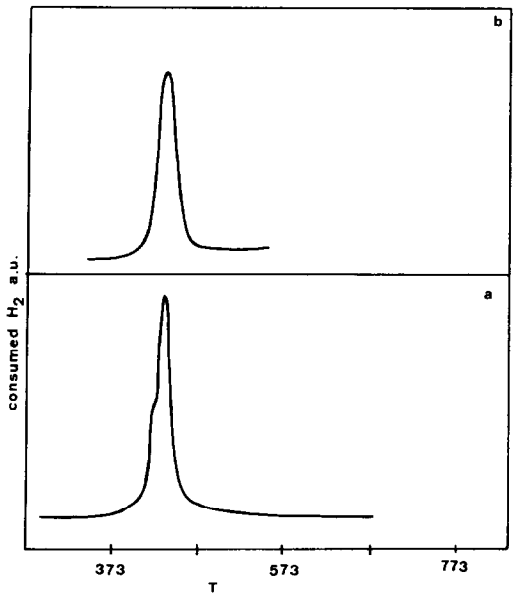

FIG. 5. Temperature-programmed reduction (TPR) experiments of (a) 0.33% sample decarbonylated *in vacuo* and oxidized at 423 K; (b) RuO_2 phase.

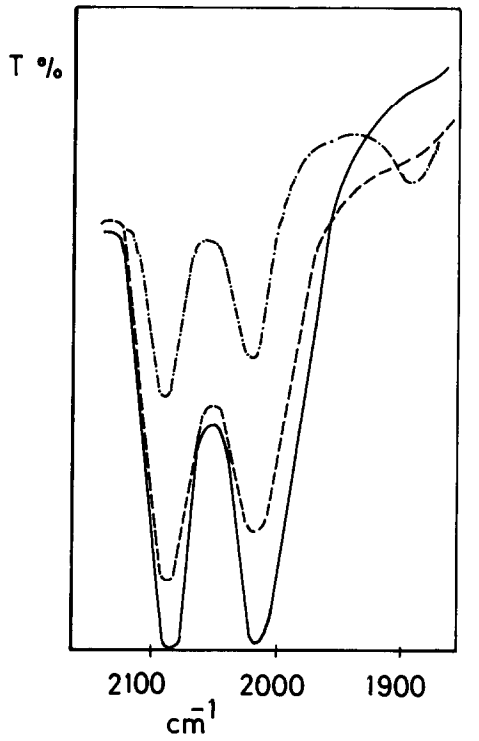

FIG. 6. Ru_B–O_2 interaction at 423 K. Solid curve: initial spectrum; dashed and dot-dashed curves: spectra taken at increasing reaction times, respectively.

illustrated in Fig. 4 can thus be considered as due to a reduction process of a RuO_2-like phase which is almost starting at the ir beam temperature. It is noticeable that both H_2 and CO tend to reduce the RuO_2 adsorbed phase at very low temperature.

The Reactivity of the Ru_B Complexes

Figure 6 shows the reaction of the Ru_B complex with O_2. At room temperature O_2 has no observable effect (within the used contact times of 20 min) on the intensity of the B pair. However, by increasing the temperature (423 K) the bands tend to disappear progressively with formation of low-frequency (1650–1200 cm^{-1}) absorbing species. At the highest oxidation stages a weak band at ~1890 cm^{-1} is formed which is destroyed by further prolonged treating in oxygen. It should be noted that the same band is also formed with similar intensity

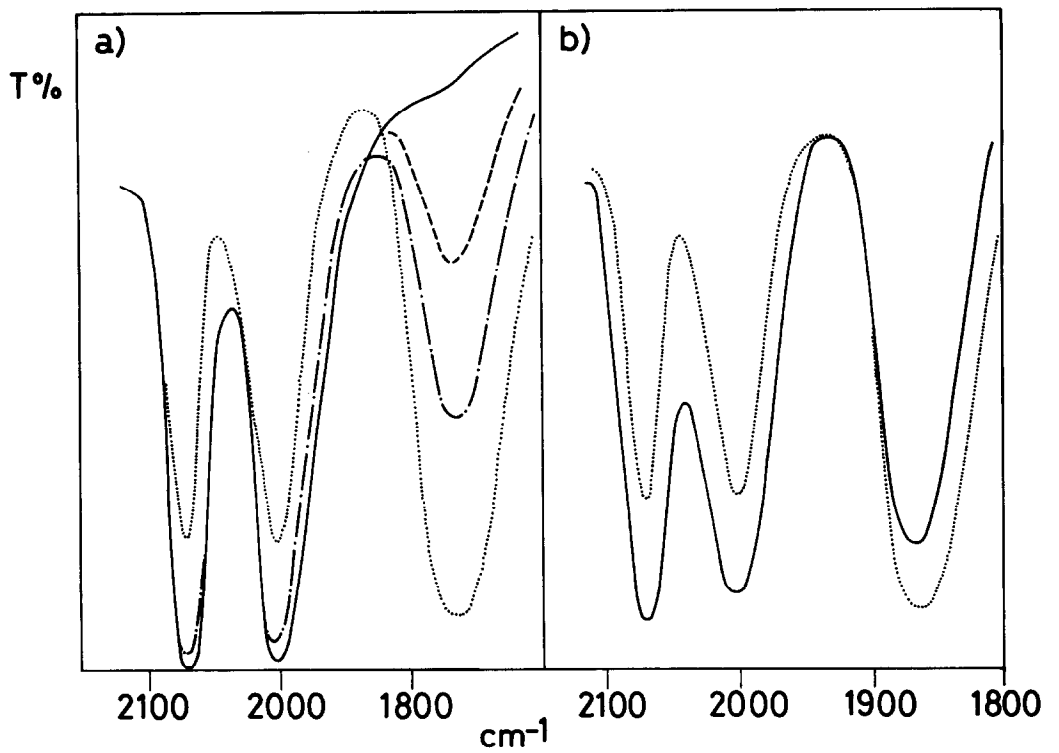

FIG. 7. Ru_B–NO interaction. (a) Solid, dot-dashed, and dotted curves: spectra taken at increasing reaction times (NO pressure 5.3 kPa). (b) solid and dotted curves: spectra taken at increasing times of the reverse process.

for R samples aged for long periods in a wet atmosphere (see Part I).

In Fig. 7a the effect of NO attack on Ru_B complexes is illustrated. It can be immediately seen that the B pair progressively declines in intensity while a nitrosylic band at 1861 cm^{-1} grows in a parallel way. This process can be reversed. Successive exposure to CO at 423 K (Fig. 7b) tends to restore the original situation.

From the interaction of NO with Ru_A complexes we have observed that NO at least partially oxidizes the ruthenium carbonylic complexes so the question arises whether the observed phenomena are due to pure ligand displacement reactions or to a more complicated process where NO acts as an oxidizing agent for the carbonylic complexes. In the latter case the nitrosylic frequency should be characteristic of NO adsorbed on oxidized ruthenium. In order to solve this question NO has been adsorbed on a sample previously oxidized in O_2. The resulting strongest NO band falls at higher frequency (1890 cm^{-1}), so a simple displacement reaction is strongly suggested.

The effect of basic ligands (Py, NH_3) has also been studied in order to reveal the presence of residual coordination vacancies or ligand displacement reactions. For the sake of brevity only the effect of pyridine is illustrated in Fig. 8, as the effect of NH_3 is nearly identical. It can be seen that Py adsorption changes continuously the frequency of the B pair towards lower frequencies. Also a very small change of the intensity ratio of the pair is observed.

The effect of hydrogen at 473 K is shown in Fig. 9: the B pair is quantitatively transformed (as demonstrated by two isosbestic points) into a new one, whose frequencies

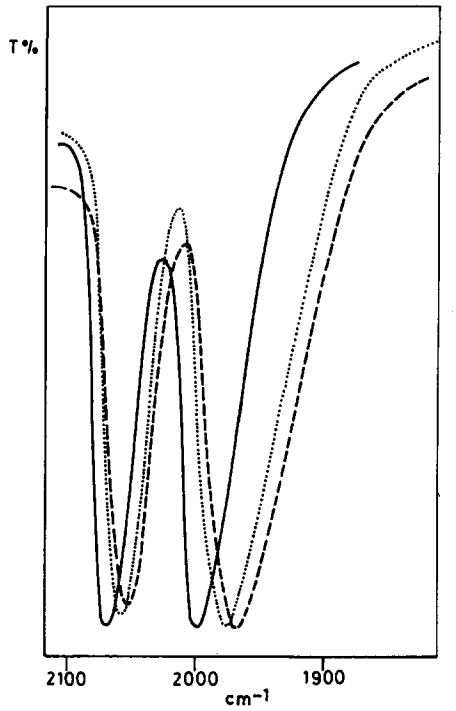

FIG. 8. Ru_B–Py interaction. Solid curve: initial spectrum; dotted and dashed curves: spectra correspond to increasing Py coverages.

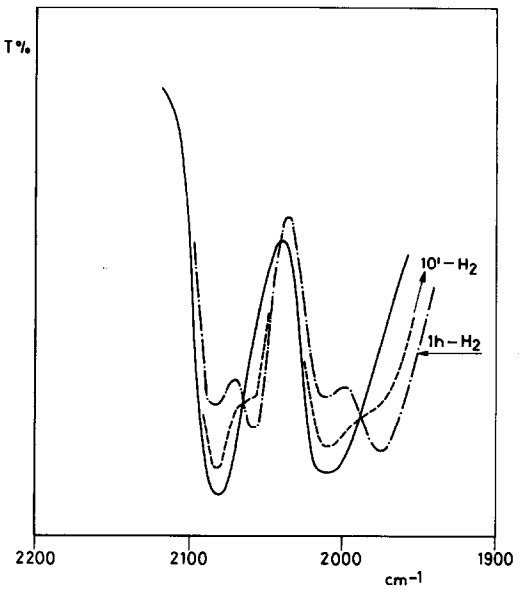

FIG. 9. Ru_B–H_2 reaction at 473 K. Solid curve: initial spectrum; dotted and dot-dashed curves; spectra taken at increasing reaction times (H_2 pressure, 5.3 kPa).

are identical to those of the C pair. This fact demonstrates that the C species contains ruthenium atoms in a more reduced form.

The Reactivity of Ru_C Complexes

Ru_C species are not easily oxidized at RT. However, if the temperature is raised to 423 K the C pair intensity declines while B species are formed (Fig. 10). This fact demonstrates that, at least partially, Ru_B and Ru_C species can be transformed one into the other under oxidizing and reducing conditions. Longer times of reaction with oxygen at 423 K cause the total disappearance of the ir bands, in agreement with the previous results which have shown that also the Ru_B complexes are oxygen sensitive at this temperature. Analogous results are obtained with NO, which initially acts as a very active oxidizing agent already at RT transforming the Ru_C species into the Ru_B species. Moreover, by increasing the

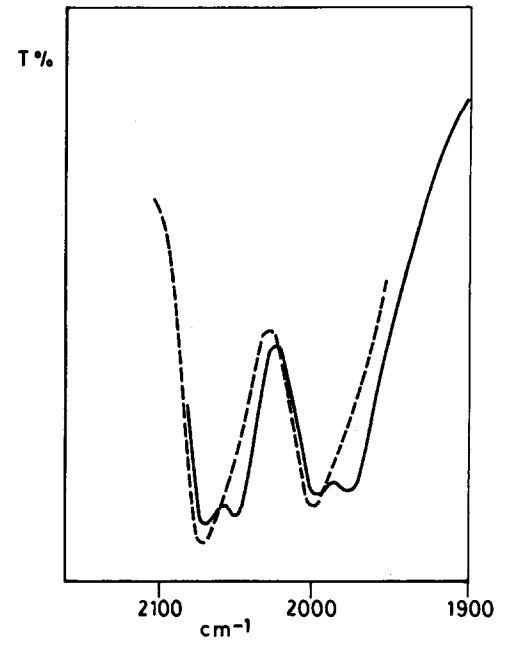

FIG. 10. Ru_C–O_2 interaction at 423 K. Solid curve: initial spectrum of Ru_B, Ru_C mixture; dashed curve: spectrum taken after interaction with O_2 (5.3 kPa) for 10 min.

contact time the reaction of NO with Ru_B complexes already described in Fig. 7 takes place.

The effect of bases (Py and NH_3) is similar to that described for the Ru_B complexes: the C pair frequencies progressively moves to lower values, but the overall shape of the spectrum does not change.

The effect of CO addition on Ru_C complexes is shown in Fig. 11. The solid line is the spectrum of a mixture of Ru_B and Ru_C complexes obtained by reduction of Ru_B species in H_2 at 473 K. Adsorption of CO at 473 K causes a decrease of the C pair, and the appearance of bands at 2138, 2075, 2045, and 2010 cm^{-1}. If the bands at 2138 and 2075 cm^{-1} are clearly due to Ru_A complexes, the others must be due to new carbonylic structures formed by addition of CO to Ru_C complexes. The presence of Ru_A complexes is not unexpected. As the reduction process is carried out at 473 K, i.e., at a temperature where Ru_A complexes are known to lose the CO ligands *in vacuo*, the initial sample contains some amount of empty unreduced Ru_A sites which successively become filled in CO atmosphere. It is most interesting that the whole process can be reversed.

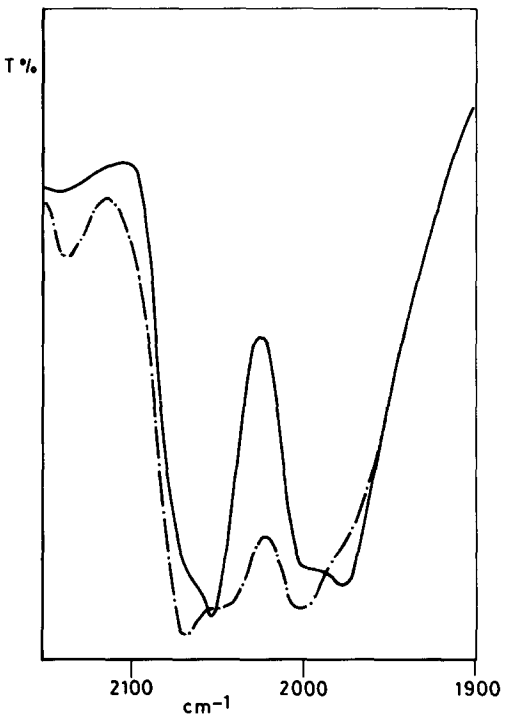

FIG. 11. Ru_C–CO interaction at 473 K. Solid curve: initial spectrum of a Ru_B–Ru_C mixture; dot-dashed curve: spectrum taken after contact with 5.3 kPa CO.

Other Reaction Tests

Other studies, concerning the chemistry of Ru_C species are in progress. In particular these complexes easily react with NH_3 and acetylene derivatives to form new surface species of unknown structure.

DISCUSSION

The Structure of the Ru_A, Ru_B, and Ru_C Species

Experiments shown in Figs. 1 and 2 demonstrate that Ru_A and Ru_B species contain two coupled linear CO oscillators. As expected, six bands are observed in both cases and their frequencies are listed in Table 1 together with those calculated on the basis of the simple Cotton–Krainhanzel model (*3*). The agreement is good, and just less satisfactory for the Ru_A species because, due to the strong overlap of the bands, the evaluation of the exact value of some of the frequencies is not possible. The existence of two isosbestic points during the formation of the Ru_C species from the Ru_B species in hydrogen demonstrates that also these species contain two coupled CO oscillators per Ru atom. Moreover, from the intensity ratios of the bands of the A, B, and C pairs the following approximate angles between the oscillators are deduced:

Ru_A	Ru_B	Ru_C
~110°	~90°	~90°

Finally, the absence for all complexes of ligand insertion with Py, NH_3, etc., indicates that the coordination sphere of the ruthenium atoms is full in all cases. On this basis tetrahedral and octahedral configurations are suggested for Ru_A and for Ru_B and Ru_C, respectively.

TABLE 1

Stretching Frequencies of Ru_A and Ru_B Complexes exchanges with ^{13}CO

ν_{CO} Ru_A complexes (cm^{-1})				ν_{CO} Ru_B complexes (cm^{-1})			
^{12}CO	^{12}CO ^{13}CO	^{13}CO	Calcd	^{12}CO	^{12}CO ^{13}CO	^{13}CO	Calcd
2134	2134		2134	2070	2070		2070
	2118		2118		2057		2060
	?	2086	2086		2022	2022	2024
2076	2076		2076	2004	2004		2004
	~2045		2044		1973		1974
	2032	2030	2030		1960	1960	1959

It must be mentioned at this point that a pair of bands very similar to those of the A pair have been observed on silica-supported ruthenium and have been assigned to dicarbonylic structures of an oxidized form of ruthenium (*4*). Kuznetsov *et al.* (*5*) have observed on a very similar system $Ru_3(CO)_{12}/\eta$-Al_2O_3, apparently correlated bands at 2130–2140, 2060–2070, and 1900–2000 cm^{-1} which have been assigned, by comparison with homogeneous $[Ru(CO)_3X_2]_n$ and $[Ru(CO)_4X_2]_n$ compounds (X = halogen), to the modes of $Ru^{II}(CO)_3$ and/or $RU^{II}(CO)_4$ groups. The first two absorptions fall at frequencies very close to those characteristic of the Ru_A species while the third one is nearly identical to the second component of the Ru_B species. As a consequence we are inclined to think that, despite some preparative differences existing between the two experiments, the three correlated absorptions mentioned before are due to a mixture of species rather than to a single one.

Ruthenium dicarbonylic species where Ru is in the divalent state are well known (*6, 7*); however, in no case were we able to find bands at frequencies as high as 2130–2140 cm^{-1}. Such high values can be understood for dicarbonylic species only if the ruthenium centre is in a higher oxidation state, in agreement with the hypothesized trivalent state. It must be mentioned at this point that CO adsorption on unreduced $RuCl_3/Al_2O_3$ and $Ru(NO)(NO_3)_3/Al_2O_3$ systems (data not yet published) gives rise to the A pair only.

As already discussed in Part I, Ru atoms in Ru_B complexes are in a lower oxidation state with respect to those in Ru_A species. Examination of the literature data of octahedral *cis*-dicarbonylic complexes of Ru^{II} (*6, 7*) shows that they are characterized by a pair of bands in the ranges 2047–2081 and 1975–2027 cm^{-1}. As the B pair falls in these two frequency intervals, the divalent state of Ru in Ru_B species, already hypothesized in Part I on the basis of pure mechanistic considerations, becomes strongly favoured.

A plausible structure for the Ru_B species is

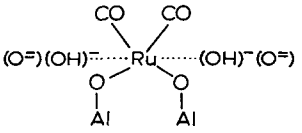

where the octahedral sphere contains $(OH)^-$ and/or O^{2-} surface ligands. At the low temperatures and loading used in this study it is quite likely that the major fraction of the Ru^{II} ions is present in groups of three. Hence the most likely result of Ru_B species reduction is the formation of metallic clusters of extremely small nuclearity, so implying that Ru_C species contain Me–Me bonds, in agreement with their characteristic absorption at ~27,000 cm^{-1} (see Part I). Of course, also in this case surface

ligands (O^{2-} and/or OH^-) are also present in the coordination sphere of the ruthenium atoms.

In order to decarbonylate Ru_C species *in vacuo* the temperature must be raised to values where an oxidative attack of the OH groups is possible with H_2 evolution. The metallic skeleton of some of the Ru_C complexes is consequently broken and the oxidized ruthenium migrates into tetrahedral positions of an aluminate or spinel-like surface structure. The preferential formation of Ru_A species on fresh samples fully decarbonylated *in vacuo* is thus easily explained. In flowing H_2 such a process is strongly inhibited and no oxidation occurs. Samples fully decarbonylated in H_2 should thus show a larger amount of zerovalent ruthenium preferentially aggregated into small microcrystals (see Part III for a more detailed discussion of this point).

The Reactivity

(*a*) *Oxidation and reduction.* All carbonylic species are oxygen sensitive at $T \geq 423$ K and this fact is not unexpected. However, the oxidized phase so formed can be reduced in CO with the initial formation of Ru_A species and subsequent generation of a mixture of more reduced surface carbonyls. It is most noticeable that anchored Ru species on zeolites with the proposed formula $Ru^I(NH_3)(CO)_2$ described by Verdonck *et al.* (*8*) and with CO stretching modes at 2020 and 2085 cm^{-1} (i.e., at frequencies very similar to those of the Ru_B species) is transformed by an oxidizing attack of water into a new monocarbonylic complex characterized by a single ir band at 1960 cm^{-1} and assigned to $Ru^{II}(NH_3)(CO)$ complexes. This observation suggests that the 1890-cm^{-1} band observed at the latest stages of the oxidation process (Fig. 6) and on R samples aged for long periods of time in wet atmosphere could be produced by parallel attack of surface water. At intermediate oxidation stages Ru_C species are transformed into the Ru_B species (Fig. 10). This process can be interpreted as the reverse of the reduction process in H_2 (Fig. 9) and confirms the parent structure proposed for these species.

(*b*) *Interaction with weak bases.* With the exception of Ru_A complexes basic molecules do not displace the CO ligands at RT. This is consistent with the lability of CO in the Ru_A groups (due to the reduced back-donation from Ru^{3+} to CO). The continuous shift of the bands of Ru_A and Ru_B pairs upon the coverage of Py (Fig. 8) can be explained as follows. Py (and other basic ligands) are adsorbed mainly on the Ru-free portion of the Al_2O_3 surface. Due to the strong dative character of the bonds formed by Py and Al^{3+} ions (*9*), inductive effects increase the negative charges on the O^{2-} and OH^- ions of the surface, thereby ultimately influencing the back-donation between CO ligands and ruthenium atoms anchored to them. The centre of gravity of the two modes is thus expected to shift to lower frequencies in agreement with the experiment. As this effect depends upon the Py (NH_3) coverage, the continuous shift of the bands is also explained. The mode at lower frequency undergoes the largest shift with coverage, showing that it responds markedly to coverage variations. This sensitivity is also responsible for the broadening effect: in fact a mode more sensitive to changes in Py coverage will also be more sensitive to heterogeneity in the environment of the Ru centres. These observations, are a clear example of induced heterogeneity as already described on other systems (*10, 11*).

(*c*) *Interaction with NO.* Although the NO–Ru_C interaction has not been described in detail it will be discussed first because of its simplicity. In the initial stages the effect of NO is to transform the Ru_C species into the Ru_B species (like oxygen). Ultimately NO decomposes on the low-valency anchored complexes as observed by several authors on reduced surfaces (*4, 12, 13*). Once the Ru_C species are oxidized to Ru_B, a second step of the reaction starts which is identical to that de-

scribed in Fig. 7. In this figure a strict proportionality between the increment of the nitrosylic band at 1861 cm^{-1} and the decrement of Ru_B carbonylic bands is observed, suggesting that the reaction must be considered as a ligand displacement where one NO displaces two CO molecules. In no cases were dinitrosylic and mixed CO–NO complexes observed. This fact cannot be easily explained. The effect of NO on Ru_A complexes is very similar: the A pair progressively decreases in intensity while a single nitrosylic absorption is observed which, at the highest coverages, reaches the 1873-cm^{-1} frequency.

We think that also in this case the main process is a displacement reaction of the CO ligands of Ru_A complexes by a single NO molecule. The slightly higher frequency of the NO stretching band reflects the higher oxidation state of the ruthenium ions of these complexes which causes the reduction of the back-donation effects. The transient shoulder at ~1810 cm^{-1} is probably due to NO adsorbed on metallic particles of Ru, as will be fully discussed in Part III of this series. It is worth mentioning that mononitrosylic complexes of Ru^{III} (*14*) show a strong ir band at 1880–1850 cm^{-1} in agreement with the previous assignment.

(*d*) *Interaction with CO.* The CO interaction with Ru_C complexes at 473 K causes dramatic changes: the C band pair tends to disappear while new bands are formed. Moreover, volumetric measurements carried out in independent experiments show that the CO/Ru ratio reaches the average value 3.0–3.5, i.e., a value intermediate between those characteristic of Ru_C and $Ru_3(CO)_{12}$ complexes and $Ru^{x+}(CO)_3$ species can be formed. These facts indicate that the system tends to restore the initial situation with formation of fully carbonylated clusters of small nuclearity. The observed increase of the CO/Ru ratio is probably accounted for by an activated ligand displacement reaction where the CO ligands displace O^{2-} and/or OH^- surface ligands. Moreover, the presence of mononuclear carbonylic complexes of the $Ru(CO)_5$ type is not excluded on the grounds of pure volumetric and spectroscopic data. These observations account for the loss of Ru from the surface occurring under high CO pressure and temperatures (*15*).

CONCLUSIONS

The complexes (Ru_A, Ru_B, and Ru_C) formed by interaction of $Ru_3(CO)_{12}$ with hydrated alumina have defined structures and reactivity. In particular:

(a) ruthenium in Ru_A species has tetrahedral configuration;

(b) ruthenium in Ru_B and Ru_C species has octahedral structure;

(c) the latter complexes can be converted one into the other by reduction and oxidation;

(d) Ru_C species probably contain Me–Me bonds;

(e) Ru_C species can adsorb CO at 473 K giving more carbonylated species of unknown structure;

(f) Ru_A and Ru_B species react with NO forming mononitrosylic species;

(g) the oxidation states of ruthenium in the three complexes are III, II, and 0, respectively.

REFERENCES

1. Zecchina, A., Guglielminotti, E., Bossi, A., and Camia, M., *J. Catal.* **74,** 225 (1982).
2. Robertson, S. D., McNicol, B. D., deBaas, J. H., Kloet, S. C., and Jekins, J. W., *J. Catal.* **37,** 424 (1975).
3. Cotton, F. A., and Krainhanzel, C. S., *J. Amer. Chem. Soc.* **84,** 4432 (1962).
4. Davydov, A. A., and Bell, A. T., *J. Catal.* **49,** 332 (1977).
5. Kuznetsov, V. L., Bell, A. T., and Yermakov, Y. I., *J. Catal.* **65,** 374 (1980).
6. Tripathi, S. C., Srivastava, S. C., Mani, R. P., and Shrimal, A. K., *Inorg. Chem. Acta Rev.* **15,** 249 (1975) and references therein.
7. Stephenson, T. A., and Wilkinson, G., *J. Inorg. Nucl. Chem.* **28,** 945 (1966); Bruce, M. I., and Stone, F. G. A., *J. Chem. Soc. A,* 1238 (1967).
8. Verdonck, J. J., Schoonheydt, R. A., and Jacobs, P. A., *in* "Proceedings, 7th International Congress on Catalysis, Tokyo, 1980," p. 911. Elsevier, Amsterdam, 1981.

9. Morterra, C., Coluccia, S., Garrone, E., and Ghiotti, G., *J. Chem. Soc. Faraday Trans. 1* **75,** 289 (1979).
10. Boccuzzi, F., Borello, E., Zecchina, A., Bossi, A., and Camia, M., *J. Catal.* **51,** 150 (1978).
11. Boccuzzi, F., Garrone, E., Zecchina, A., Bossi, A., and Camia, M., *J. Catal.* **51,** 160 (1978).
12. Davydov, A. A., and Bell, A. T., *J. Catal.* **49,** 345 (1977).
13. Brown, M. F., and Gonzales, R., *J. Catal.* **44,** 477 (1978).
14. Connelly, N. G., *Inorg. Chim. Acta Rev.* **6,** 47, (1972).
15. Bossi, A., unpublished data.